Inorg. Chem. **2003**, *42*, 205–209

Syntheses, Structures, and Characterization of New Lead(II)–Tellurium(IV)–Oxide Halides: $Pb_3Te_2O_6X_2$ and $Pb_3TeO_4X_2$ (X = Cl or Br)

Yetta Porter and P. Shiv Halasyamani*

Department of Chemistry, University of Houston, 4800 Calhoun Boulevard, Houston, Texas 77204-5003

Received May 24, 2002

The syntheses, structures, and characterization of four new lead(II)–tellurium(IV)–oxide halides, $Pb_3Te_2O_6X_2$ and $Pb_3TeO_4X_2$ (X = Cl or Br) are reported. The materials are synthesized by solid-state techniques, using $Pb_3O_2Cl_2$ or $Pb_3O_2Br_2$ and TeO_2 as reagents. The compounds have three-dimensional structural topologies consisting of lead–oxide halide polyhedra connected to tellurium oxide groups. In addition, the Pb^{2+} and Te^{4+} cations are in asymmetric coordination environments attributable to their stereoactive lone pair. We also demonstrate that $Pb_3Te_2O_6X_2$ and $Pb_2TeO_4X_2$ can be interconverted reversibly through the loss or addition of TeO_2. X-ray data: $Pb_3Te_2O_6Cl_2$, monoclinic, space group *C*2/*m* (No. 12), $a = 16.4417(11)$ Å, $b = 5.6295(4)$ Å, $c = 10.8894(7)$ Å, $\beta = 103.0130(10)°$, $Z = 4$; $Pb_3Te_2O_6Br_2$, monoclinic, space group *C*2/*m* (No. 12), $a = 16.8911(8)$ Å, $b = 5.6804(2)$ Å, $c = 11.0418(5)$ Å, $\beta = 104.253(2)°$, $Z = 4$; $Pb_3TeO_4Cl_2$, orthorhombic, space group *Bmmb* (No. 63), $a = 5.576(1)$ Å, $b = 5.559(1)$ Å, $c = 12.4929(6)$ Å, $Z = 4$; $Pb_3TeO_4Br_2$, orthorhombic, space group *Bmmb* (No. 63), $a = 5.6434(4)$ Å, $b = 5.6434(5)$ Å, $c = 12.9172(6)$ Å, $Z = 4$.

Introduction

The interest in synthesizing new mixed-metal oxide halide materials exists not only for their potential ion-exchange behavior but also for their optical properties as well as interesting crystal chemistry. We have previously reported that a low-temperature (160 °C) aqueous method can be employed for the synthesis of new metal oxide halides.[1] Specifically, we synthesized and characterized $Pb_3(SeO_3)(SeO_2OH)Cl_3$ and $Pb_3(SeO_3)_2Cl_2$ utilizing this reflux technique and demonstrated that an irreversible transformation occurs between the two materials with the loss of HCl. In this paper, we report the syntheses, structures, and characterization of new Pb(II)−Te(IV)−oxide halides, $Pb_3Te_2O_6X_2$ and $Pb_3TeO_4X_2$ (X = Cl or Br). In addition, we demonstrate that a reversible transformation occurs between the two materials through the loss or addition of TeO_2.

Experimental Section

Reagents. PbO (99.9+ %, Aldrich), $PbCl_2$ (99%, Alfa Aesar), and TeO_2 (99.9% Aldrich) were used as received. $Pb_3O_2Cl_2$ and $Pb_3O_2Br_2$ were synthesized by heating a stoichiometric mixture of PbO and the corresponding lead halide in air at 500 °C for 1 day. The powder X-ray diffraction patterns for $Pb_3O_2Cl_2$ and $Pb_3O_2Br_2$ matched those previously reported.[2−4]

Synthesis. Single crystals of $Pb_3Te_2O_6Cl_2$ were grown by combining $Pb_3O_2Cl_2$ (0.2658 g, 3.67×10^{-4} mol) and TeO_2 (0.2342 g, 1.47×10^{-3} mol) in a fused silica tube that was subsequently evacuated and sealed. The mixture was heated at 550 °C for 1 day and cooled at a rate of 6 °C h^{-1} to room temperature. A few clear colorless crystals were observed (roughly 2% of the bulk powder). Bulk, polycrystalline $Pb_3Te_2O_6Cl_2$ was synthesized by combining $Pb_3O_2Cl_2$ (0.3466 g, 4.79×10^{-4} mol) and TeO_2 (0.1529 g, 9.58×10^{-4} mol). The mixture was introduced into a fused silica tube that was subsequently evacuated and sealed. The tube was heated to 575 °C for 1 day and then furnace cooled to room temperature. An off-white powder was recovered.

The other phases, $Pb_3Te_2O_6Br_2$, $Pb_3TeO_4Cl_2$, and $Pb_3TeO_4Br_2$, were synthesized as polycrystalline powders. All attempts to grow single crystals were unsuccessful. Each material was synthesized by combining stoichiometric amounts of $Pb_3O_2Br_2$ ($Pb_3O_2Cl_2$) with TeO_2. The mixtures were introduced into separate fused silica tubes

* To whom correspondence should be addressed. E-mail: psh@uh.edu.

(1) Porter, Y.; Halasyamani, P. S. *Inorg. Chem.* **2001**, *40*, 2640.
(2) Vincent, H.; Perrault, G. *Bull. Soc. Fr. Mineral. Cristallogr.* **1971**, *94*, 323.
(3) Berdonosov, P. S.; Dolgikh, V. A.; Popovkin, B. A. *Mater. Res. Bull.* **1996**, *31*, 717.
(4) Pasero, M.; Vacchiano, D. *Neues Jahrb. Mineral., Monatsh.* **2000**, 563−569.

10.1021/ic025750j CCC: $25.00
Published on Web 12/05/2002

Table 1. Crystallographic Data for $Pb_3Te_2O_6Cl_2$

fw	1043.67
space group	*C*2/*m* (No. 12)
a (Å)	16.4417(11)
b (Å)	5.6295(4)
c (Å)	10.8894(7)
β (deg)	103.013(10)
V (Å^3)	982.02(11)
Z	4
temp (°C)	25.0(2)
λ (Å)	0.71073
ρ (g cm^{-3})	7.059
μ (cm$^{-1)}$	576.65 cm^{-1}
$R(F)^a$	0.0617
$R_w(F^2)^b$	0.158

^{a} $R = \Sigma||F_o| - |F_c||/\Sigma|F_o|$. ^{b} $R_w = [\Sigma w(|F_o^2| - |F_c^2|)^2/\Sigma w(F_o^2)^2]^{1/2}$.

that were subsequently evacuated and sealed. For $Pb_3Te_2O_6Br_2$ ($Pb_3TeO_4Cl_2$ and $Pb_3TeO_4Br_2$) the tubes were heated to 575 °C (650 °C) for 1 day and cooled at a rate of 6 °C h^{-1} to room temperature. With $Pb_3Te_2O_6Br_2$ ($Pb_3TeO_4Cl_2$ and $Pb_3TeO_4Br_2$) off-white (yellow) polycrystalline powders were recovered.

Single-Crystal Structure Determination. The structure of $Pb_3Te_2O_6Cl_2$ was determined by standard crystallographic methods. For $Pb_3Te_2O_6Cl_2$ a colorless column (0.04 mm × 0.08 mm × 0.20 mm) was used for single-crystal measurements. Room-temperature intensity data were collected on a Siemens SMART diffractometer equipped with a 1K CCD area detector using graphite- monochromated Mo Kα radiation. A hemisphere of data was collected using a narrow-frame method with scan widths of 0.30° in ω and an exposure time of 25 s/frame. The first 50 frames were remeasured at the end of the data collection to monitor instrument and crystal stability. The maximum correction applied to the intensities was <1%. The data were integrated using the Siemens SAINT program,[5] with the intensities corrected for Lorentz, polarization, air absorption, and absorption attributable to the variation in the path length through the detector faceplate. ψ-scans were used for the absorption correction on the hemisphere of data. The data were solved and refined using SHELXS-97 and SHELXL-97, respectively.[6,7] All calculations were performed using the WinGX-98 crystallographic software package.[8] Crystallographic data, atomic coordinates, and thermal parameters for $Pb_3Te_2O_6Cl_2$ are given in Tables 1 and 2.

Powder Diffraction and Crystal Structure Refinement. The X-ray powder diffraction data were collected on a Scintag XDS2000 diffractometer at room temperature (Cu Kα radiation, $\theta-\theta$ mode, flat plate geometry) in the 2θ range 3−110° with a step size of 0.02° and a step time of 10 s. The diffraction patterns were analyzed using the Rietveld[9] method with the FULLPROF program.[10] An asymmetry correction was applied to the low-angle reflections. The scale was refined initially, followed in subsequent iterations by the zero point error, cell constants, peak shape parameters, atomic parameters, and overall isotropic temperature factors. For $Pb_3Te_2O_6Cl_2$, a powder refinement was undertaken attributable to the somewhat large errors observed in the single-crystal refinement.

(5) *SAINT*, version 4.05 ed.; Siemens Analytical X-ray Systems, Inc.: Madison, WI, 1995.
(6) Sheldrick, G. M. *SHELXS-97-A program for automatic solution of crystal structures*; University of Goettingen: Goettingen, Germany, 1997.
(7) Sheldrick, G. M. *SHELXL-97-A program for crystal structure refinement*; University of: Goettingen: Goettingen, Germany, 1997.
(8) Farrugia, L. J. WinGX: An integrated system of publically available windows programs for the solution, refinement, and analysis of single-crystal X-ray diffraction data. *J. Appl. Crystallogr.* **1998**, *32*, 837.
(9) Rietveld, H. M. *J. Appl. Crystallogr.* **1969**, *2*, 65.
(10) Rodriguez, J. C. *FULLPROF Program: Rietveld Pattern Matching Analysis of Powder Patterns*; ILL: Grenoble, France, 1990.

Table 2. Atomic Coordinates for $Pb_3Te_2O_6Cl_2$

atom	*x*	*y*	*z*	$U_{eq}{}^a$ (Å^2)
Pb(1)	0.26200(6)	0.0000	0.20191(9)	0.0113(4)
Pb(2)	0.02126(6)	0.0000	0.20025(9)	0.0108(4)
Pb(3)	0.16092(7)	0.5000	0.39346(10)	0.0145(4)
Te(1)	0.10312(10)	0.5000	0.05086(15)	0.0088(4)
Te(2)	0.37188(10)	0.5000	0.40736(15)	0.0088(4)
Cl(1)	0.3179(4)	0.5000	0.0993(6)	0.0166(14)
Cl(2)	−0.0410(5)	0.5000	0.3016(8)	0.0252(17)
O(1)	0.1309(8)	0.263(3)	0.1830(12)	0.016(3)
O(2)	0.0000	0.288(4)	0.0000	0.024(5)
O(3)	0.3935(13)	0.5000	0.5810(19)	0.018(2)
O(4)	0.2913(9)	0.262(3)	0.3859(13)	0.018(2)

^{a} U_{eq} is defined as one-third of the trace of the orthogonalized $\mathbf{U}_{ij}$ tensor.

Table 3. Summary of Crystallographic Powder X-ray Diffraction and Refinement Data for $Pb_3Te_2O_6Cl_2$ and $Pb_3TeO_4Cl_2$

	$Pb_3Te_2O_6Cl_2$	$Pb_3TeO_4Cl_2$
a (Å)	16.4349(5)	5.576(1)
b (Å)	5.6255(1)	5.559(1)
c (Å)	10.8802(3)	12.4929(6)
β (deg)	103.050(1)	
V (Å^3)	979.94(1)	385.9(1)
space group	*C*2/*m* (No. 12)	*Bmmb* (No. 63)
observns	1380	352
χ^2	2.55	3.25
$R_p{}^a$	0.131	0.169
$R_{wp}{}^b$	0.167	0.215
$R_{exp}{}^c$	0.104	0.119
$R_{Bragg}{}^d$	0.069	0.087

^{a} $R_p = \Sigma|I_o - I_c|/\Sigma I_o$. ^{b} $R_{wp} = [\Sigma w|I_o - I_c|^2/\Sigma w I_o^2]^{1/2}$. ^{c} $R_{exp} = R_{wp}/(\chi^2)^{1/2}$. ^{d} $R_{Bragg} = \Sigma|I_{k(obs)} - I_{k(calc)}|/\Sigma I_{k(obs)}$, where I_o and I_c are the observed and calculated integrated intensities, I_k is the Bragg intensity, and w is the weight derived from an error propagation scheme during the process of the least-squares refinement.

The peaks were indexed on a monoclinic cell, with the refinements of the unit cell constants performed using a least-squares method. The structural refinements were carried out in space group *C*2/*m* (No. 12) with a starting model based on the single-crystal data. A total of 44 parameters, including 13 profile parameters, were used in the refinement. For $Pb_3TeO_4Cl_2$ the peaks were indexed on an orthorhombic cell, with refinement of the unit cell constants performed by a least-squares method. The structural refinements were carried out in space group *Bmmb* (No. 63) with a starting model based on the structure of orthorhombic $PbBiO_2Cl$. To model $Pb_3TeO_4Cl_2$ with the orthorhombic $PbBiO_2Cl$ structure, statistical disorder must occur between the Pb^{2+} and the Te^{4+} cations. A variety of disorder models are possible; however, the model that gave the best fit to the data and made the most chemical sense is to statistically disorder Pb(2) and Te(1) (vide infra). In addition, although the unit cell is metrically tetragonal, refinements using higher symmetry tetragonal space groups resulted in large errors. A total of 20 parameters, including 12 profile parameters, were used in the refinement. The results of the powder refinements, atomic coordinates, thermal parameters, and bond distances are given in Tables 3−5. $Pb_3Te_2O_6Br_2$ and $Pb_3TeO_4Br_2$ are isostructural with $Pb_3Te_2O_6Cl_2$ and $Pb_3TeO_4Cl_2$, respectively. Tables 6 and 7 gives the refined unit cell, space group, *hkl*, d_{obs}, d_{calc}, I_{obs}, and I_{calc} for $Pb_3Te_2O_6Br_2$ and $Pb_3TeO_4Br_2$, respectively.

Infrared Spectroscopy. Infrared spectra were recorded on a Matteson FTIR 5000 spectrometer in the 400−4000 cm^{-1} range, with the sample pressed between two KBr pellets.

Thermogravimetric Analysis. Thermogravimetric measurements were carried out on a TGA 2950 thermogravimetric analyzer (TA Instruments). The samples were contained within platinum

Table 4. Fractional Atomic Coordinates, Isotropic Temperature Factors (Å^2), and Occupancies for $Pb_3TeO_4Cl_2$

atom	*x*	*y*	*z*	U_{eq} (Å^2)	occ
Pb(1)	0.00000	0.2500	0.39063(19)	0.02504(9)	1.0
Pb(2)	0.00000	0.2500	0.09796(23)	0.0219(1)[a]	0.5
Te(1)	0.00000	0.2500	0.09796(23)	0.0219(1)[a]	0.5
Cl(1)	0.00000	0.2500	0.74746(114)	0.0123(30)	1.0
O(1)	0.767(3)	0.0000	0.00000	0.0116(58)	1.0

[a] These atoms were constrained to have the same atomic coordinates and thermal parameters.

Table 5. Selected Bond Distances (Å) for $Pb_3Te_2O_6Cl_2$[a] and $Pb_3TeO_4Cl_2$[b]

	$Pb_3Te_2O_6Cl_2$		
Pb(1)−O(1)	2.586(14) × 2	Pb(2)−Cl(2)	3.270(12) × 2
Pb(1)−O(4)	2.447(15) × 2	Pb(3)−O(1)	2.600(14) × 2
Pb(1)−Cl(1)	3.237(12)	Pb(3)−O(4)	2.544(16) × 2
Pb(1)−Cl(2)	3.176(12)	Pb(3)−O(4)	2.778(15) × 2
Pb(2)−O(1)	2.374(14) × 2	Pb(3)−O(3)	2.985(15) × 2
Pb(2)−O(2)	2.677(13) × 2	Pb(3)−Cl(2)	3.244(12)
Pb(2)−O(3)	2.48(2)		
Te(1)−O(1)	1.938(13) × 2	Te(2)−O(3)	1.84(2)
Te(1)−O(2)	2.044(12) × 2	Te(2)−O(4)	1.861(16) × 2
	$Pb_3TeO_4Cl_2$		
Pb(1)−O(1)	2.452(12) × 4	Pb(1)−Cl(1)	3.305(12) × 2
Pb(1)−Cl(1)	3.271(12) × 2	Pb(2)/Te(2)−O(1)	2.257(12) × 4

[a] Single-crystal data. [b] Powder diffraction data.

Table 6. Powder XRD Data for $Pb_3Te_2O_6Br_2$[a]

h	*k*	*l*	d_{calc}	d_{obs}	I_{calc}	I_{obs}
2	0	0	8.186	8.231	2	3
−2	0	1	7.446	7.486	13	14
0	0	2	5.351	5.369	5	5
−4	0	1	4.182	4.190	9	8
3	1	0	3.935	3.941	10	10
−4	0	2	3.723	3.723	1	1
1	1	2	3.645	3.651	27	26
−2	0	3	3.612	3.625	2	1
4	0	1	3.543	3.458	1	1
−3	1	2	3.479	3.484	8	9
−1	1	3	3.088	3.092	100	100
4	0	2	2.922	2.925	43	42
−5	1	1	2.899	2.903	97	92
1	1	3	2.866	2.870	4	4
0	2	0	2.840	2.843	50	47
−6	0	1	2.815	2.826	2	3
−2	0	4	2.751	2.758	1	1
0	0	4	2.675	2.678	1	1
5	1	1	2.608	2.612	4	4
−4	0	4	2.545	2.543	2	2
0	2	2	2.509	2.510	2	1
−1	1	4	2.476	2.480	1	1
4	0	3	2.411	2.414	2	2
−4	2	1	2.350	2.352	3	3
1	1	4	2.321	2.322	2	2
−4	2	2	2.258	2.259	1	1

[a] Refined unit cell a = 16.8911(8) Å, b = 5.6804(2) Å, c =11.0418(5) Å, and β = 104.253(2)° and space group *C*2/*m* (No. 12).

crucibles and heated at a rate of 2 °C min^{-1} from room temperature to 900 °C in flowing nitrogen.

Results and Discussion

The isostructural materials $Pb_3Te_2O_6Cl_2$ and $Pb_3Te_2O_6Br_2$ have three-dimensional structural topologies consisting of lead−oxide halide polyhedra linked to tellurium−oxide groups (see Figures 1and 2). In both materials the Pb^{2+} cations are linked to both oxygen and chloride (bromide)

Table 7. Powder XRD Data for $Pb_3TeO_4Br_2$[a]

h	k	l	d_{calc}	d_{obs}	I_{calc}	I_{obs}
0	0	2	6.459	6.490	4	5
1	1	1	3.812	3.822	19	18
1	1	3	2.927	2.932	100	100
0	2	0	2.822	2.826	21	18
1	1	5	2.169	2.171	2	2
0	0	6	2.153	2.156	6	7
0	2	4	2.125	2.128	6	7
0	1	6	1.995	1.997	18	22
1	3	1	1.768	1.768	2	3
0	2	6	1.712	1.722	8	6
2	0	6	1.711	1.713	7	6
2	2	4	1.697	1.699	4	5
1	1	7	1.675	1.677	7	6
1	3	3	1.649	1.650	16	18
0	0	8	1.615	1.617	1	4
2	2	6	1.463	1.469	7	15
4	0	0	1.411	1.412	3	3
0	2	8	1.401	1.402	1	1

[a] Refined unit cell a = 5.6434(4) Å, b = 5.6434(5) Å, and c =12.9172(6) Å and space group *Bmmb* (No. 63).

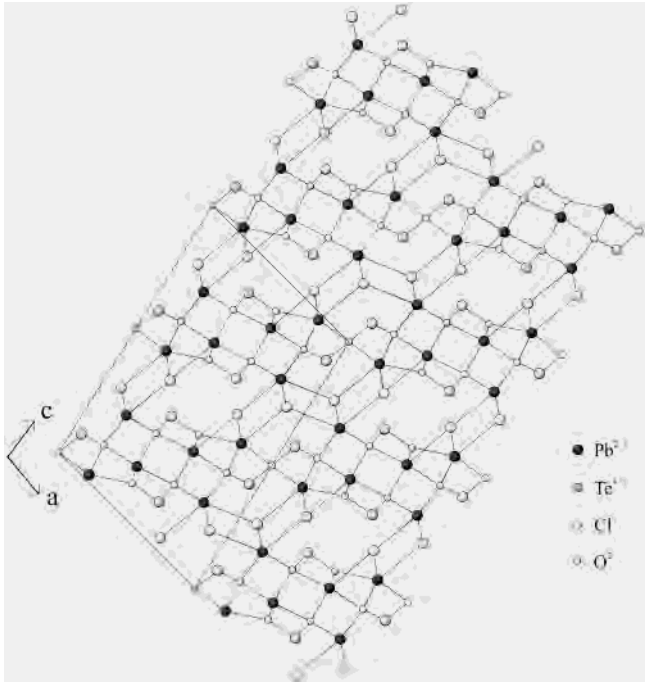

Figure 1. Ball-and-stick diagram of $Pb_3Te_2O_6Cl_2$ in the $a-c$ plane.

forming $PbO_4Cl_4(Br_4)$, $PbO_5Cl_3(Br_3)$, and $PbO_8Cl(Br)$ groups for Pb(1), Pb(2), and Pb(3), respectively, whereas the Te^{4+} cations are only bonded to oxygen forming TeO_4 and TeO_3 groups for Te(1) and Te(2), respectively. Both Pb^{2+} and Te^{4+} are in highly asymmetric coordination environments attributable to their stereoactive lone pair. The lone pairs point into the layer, between the halide anions. The Pb−O and Pb−Cl bond distances range 2.447(15)−2.994(15) and 3.236(12)−3.270(12) Å, respectively, whereas the Te−O bond distances range 1.84(2)−2.044(12) Å. The closest Te−Cl contacts are at a distance of greater than 3.2 Å. Bond valence sums[11,12] for Pb^{2+} range from 1.83 to 2.19 and for Te^{4+} are 3.89 and 4.18.

(11) Brown, I. D.; Altermatt, D. *Acta Crystallogr.* **1985**, *B41*, 244.
(12) Brese, N. E.; O'Keeffe, M. *Acta Crystallogr.* **1991**, *B47*, 192.

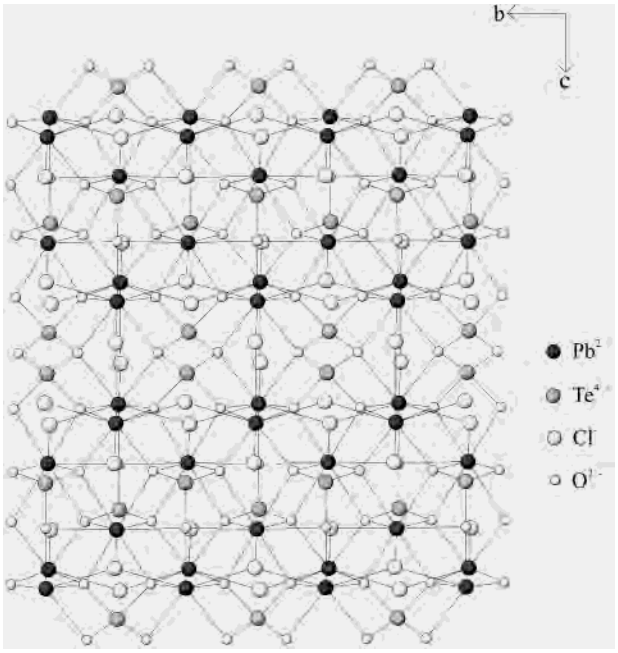

Figure 2. Ball-and-stick diagram of $Pb_3Te_2O_6Cl_2$ in the $b-c$ plane.

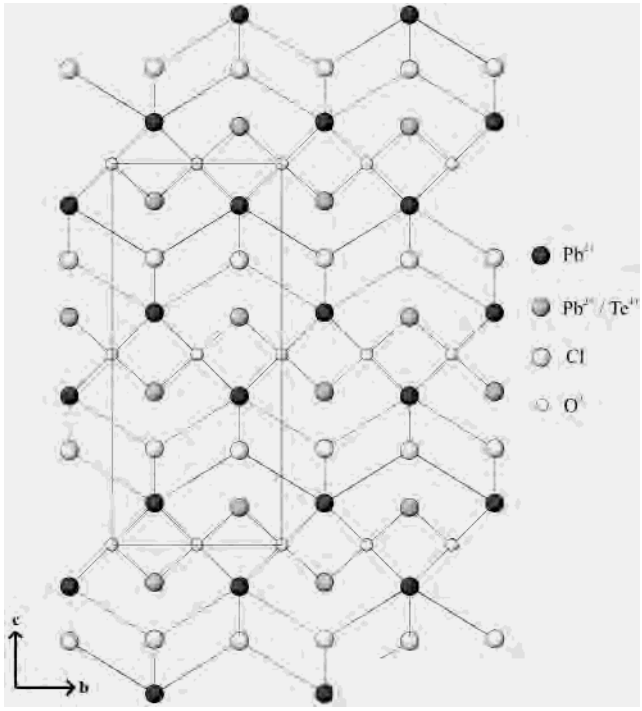

Figure 3. Ball-and-stick diagram of $Pb_3TeO_4Cl_2$ in the $b-c$ plane. Note the large, clear spheres are statistically disordered between Pb^{2+} and Te^{4+}.

$Pb_3TeO_4Cl_2$ and $Pb_3TeO_4Br_2$ also have three-dimensional structural topologies with lead−oxide halide polyhedra linked to tellurium oxide groups (see Figure 3). The materials are isostructural with orthorhombic $PbBiO_2Cl$[13] and $PbSbO_2Cl$ (Nadorite).[14−16] The Pb−O bond distances are 2.452(12) Å with Pb−Cl bond distances of 3.274(12) and 3.305(12) Å, whereas the Te−O bond distances are 2.252(12) Å. Similar to $Pb_3Te_2O_6Cl_2$, the closest Te−Cl contacts are greater than 3.2 Å. The relationship between the stoichiometries of $PbBiO_2Cl$ and $Pb_3TeO_4Cl_2$ may be understood as follows. If the formula of $PbBiO_2Cl$ is "doubled", "$Pb_2Bi_2O_4Cl_2$" is obtained. If the two Bi^{3+} cations are replaced by one Te^{4+} and one Pb^{2+} cation, "$Pb_2(PbTe)O_4Cl_2$" ≡ $Pb_3TeO_4Cl_2$ may be formulated. As stated earlier the Te^{4+} can be disordered over both Pb^{2+} sites, without any detriment to the refinement. However, this would result in larger, chemically unreasonable, Te−O bond lengths (ca. 2.452(12) Å). Thus, we decided to statistically disorder Pb(2) and Te(1) resulting in four equal Te−O bonds distances of 2.257(12) Å (see Tables 4 and 5).

Table 8. Infrared Spectroscopy Data (cm^{-1}) for $Pb_3Te_2O_6X_2$ and $Pb_3TeO_4X_2$ (X = Cl or Br)

	ν(Pb−O)		ν(Te−O)			ν(Te−O−Pb)
$Pb_3Te_2O_6Cl_2$	701	534	750	669	636	422
$Pb_3Te_2O_6Br_2$	696	522	746	659	632	416
$Pb_3TeO_4Cl_2$		509		661	628	439
$Pb_3TeO_4Br_2$		499		653	613	441

Infrared Spectroscopy. The infrared spectra for $Pb_3Te_2O_6Cl_2$, $Pb_3Te_2O_6Br_2$, $Pb_3TeO_4Cl_2$, and $Pb_3TeO_4Br_2$ revealed a host of Pb−O, Te−O, and Te−O−Pb vibrations. Table 8 summarizes the infrared data. The additional Pb−O and Te−O stretches observed in $Pb_2Te_2O_6X_2$ compared with $Pb_2TeO_4X_2$ are attributable to the different coordination environments of the Pb^{2+} and Te^{4+} cations in the materials. In $Pb_2Te_2O_6X_2$ the Pb^{2+} are in 8- and 9-fold coordination environments, whereas in $Pb_2TeO_4X_2$ the Pb^{2+} is only in an 8-fold environment. Similarly for Te^{4+}, in $Pb_2Te_2O_6X_2$ the Te^{4+} are in 3- and 4-fold environments, whereas in $Pb_2TeO_4X_2$ the Te^{4+} is only in a 3-fold environment. All of the assignments are consistent with those previously reported.[17−19]

Thermogravimetric Measurements. For $Pb_3Te_2O_6Cl_2$ ($Pb_3Te_2O_6Br_2$), the TGA measurements revealed one transition between 560 and 750 °C corresponding to a weight loss of 15.57% (14.21%). The weight loss is consistent with the following reaction:

$$Pb_3Te_2O_6X_2 \rightarrow Pb_3TeO_4X_2 + TeO_2\uparrow$$

Here X = Cl or Br. The calculated weight loss for this reaction for $Pb_3Te_2O_6Cl_2$ ($Pb_3Te_2O_6Br_2$) is 15.29% (14.09%). For $Pb_3TeO_4Cl_2$ ($Pb_3TeO_4Br_2$), the TGA measurements also revealed one transition between 650 and 850 °C corresponding to a weight loss of 31.46% (37.62%). The weight loss is consistent with the following reaction:

$$Pb_3TeO_4X_2 \rightarrow Pb_2TeO_4 + PbCl_2\uparrow$$

Here X = Cl or Br. The calculated weight loss for this reaction for $Pb_3TeO_4Cl_2$ ($Pb_3TeO_4Br_2$) is 31.81% (37.72%).

One of the most interesting aspects of the reported materials is their interconvertibility. As demonstrated by the TGA measurements, when $Pb_3Te_2O_6Cl_2$ is heated above 560

(13) Gillberg, M. *Arkiv Mineral. Geol.* **1961**, *2*, 565.
(14) Sillen, L. G.; Melander, L. *Z. Kristallogr.* **1941**, *103*, 420.
(15) Giuseppetti, G.; Tadini, C. *Period. Mineral.* **1973**, *42*, 335.
(16) Porter, Y.; Halasyamani, P. S. *Z. Naturforsch.* **2002**, *57b*, 360.
(17) Brooker, M. H.; Irish, D. E. *J. Chem. Phys.* **1970**, *53*, 1083.
(18) Bart, J. C. J.; Petrini, G. Z. *Z. Anorg. Allg. Chem.* **1984**, *509*, 183.
(19) Nakamoto, K. *Infrared and Raman Spectra of Inorganic and Coordination Compounds*, 5th ed.; John Wiley & Sons: 1997.

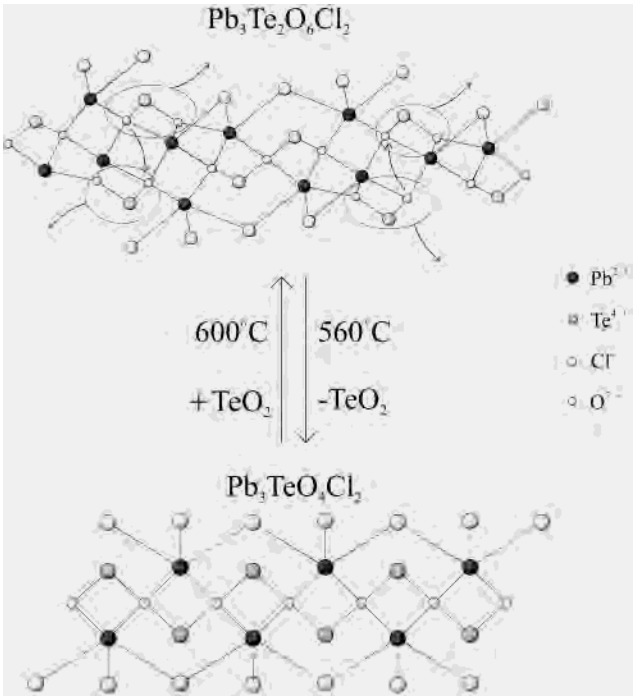

Figure 4. Schematic structural representation of the interconversion between $Pb_3Te_2O_6Cl_2$ and $Pb_3TeO_4Cl_2$. The circled atoms indicate where TeO_2 may be lost, or added, during the transformation.

°C, the material loses TeO_2 and forms $Pb_3TeO_4Cl_2$. Interestingly, when $Pb_3TeO_4Cl_2$ is combined with TeO_2 and heated in an evacuated and sealed quartz tube at 600 °C for 12 h, $Pb_3Te_2O_6Cl_2$ is re-formed. The interconversion, which also occurs with the bromine analogues, indicates a great deal of stability in the lead(II)−tellurium(IV)−oxide "sheets". The aforementioned reaction is outlined below, and Figure 4 gives a schematic structural representation of the loss, or addition, of TeO_2 between $Pb_3Te_2O_6Cl_2$ and $Pb_3TeO_4Cl_2$.

$$Pb_3Te_2O_6Cl_2 \underset{+TeO_2,\ 600\ °C}{\overset{-TeO_2,\ 560\ °C}{\rightleftharpoons}} Pb_3TeO_4Cl_2$$

Conclusion. We have reported the synthesis and characterization of four new mixed-metal oxide halide materials, $Pb_3Te_2O_6X_2$ and $Pb_3TeO_4X_2$ (X = Cl or Br). All of the materials have three-dimensional structural topologies, with lead−oxide halide polyhedra linked to tellurium−oxide groups. The stereoactive lone pairs on the Pb^{2+} and Te^{4+} point into the layer, between the halide anions. Interestingly, the materials may be interconverted through the loss or addition of TeO_2. Synthetically, we prepared all the reported materials by a combination of an oxide halide, $Pb_3O_2X_2$ (X = Cl or Br), and an oxide, TeO_2. This suggests that other three-dimensional materials are possible. We are pursuing this avenue of synthetic research and will be reporting on the new materials shortly.

Acknowledgment. We wish to thank the reviewers for perceptive criticism of an earlier version of the manuscript. We thank the Robert A. Welch Foundation for support. We wish to acknowledge the Center for Materials Chemistry at the University of Houston (CMC-UH) for support. This work was also supported by the NSF-Career Program through Grant DMR-0092054, and an acknowledgment is made to the donors of the Petroleum Research Fund, administered by the American Chemical Society, for partial support of this research. P.S.H. is a Beckman Young Investigator.

Supporting Information Available: Refined powder X-ray diffraction patterns for $Pb_3Te_2O_6Cl_2$ and $Pb_3TeO_4Cl_2$ and a CIF for $Pb_3Te_2O_6Cl_2$. This material is available free of charge via the Internet at http://pubs.acs.org.

IC025750J